(averaged) fluorine. In structures **22**–**28**, A, A′, B, and B′ indicate distinguishable methyl groups.

The diethoxy compound **26** shows three different temperature regions.[26] First, below −68°, there are only two ring methyl groups and this is interpreted as evidence for the same aeae process as in **22** ⇄ **23**. Above −20°, the two methyl peaks coalesce while the ABM_3X spectrum of the CH_3CH_2OP group remains unchanged, a result which is interpreted as evidence for the rearrangement going through the analog of **25**. The high-temperature equilibration of all the protons is interpreted as going through the analog of **24**. The low-temperature experiment can also be interpreted as evidence for the analog of **25** with the intermediate result the same as above except that now the excitation is to the analog of **22** ⇄ **23**. Another interpretation of the high-temperature experiment would describe the rearrangement as an aexae process taking **26** to **27**. Since the low-temperature nmr spectrum shows rearrangement of **26** ⇄ **28**, the combination of the two rearrangements aeae and aexae would serve to equilibrate all the CH_2 peaks as is observed.

Most examples of $RR'SF_4$ compounds show R and R′ to be cis as in[26] **29** and the only reported example,

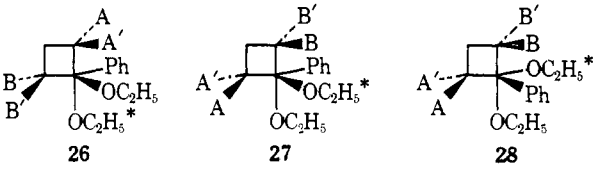

26 **27** **28**

which shows identical fluorine atoms, can be interpreted not only as a rigid molecule[27] with trans substituents as in **30** but also as the cis complex **31** under-

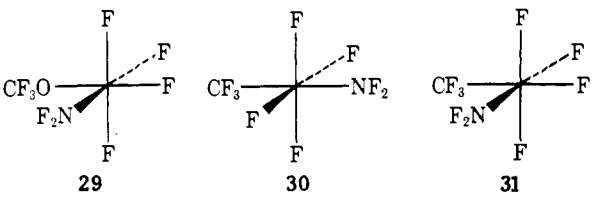

29 **30** **31**

going rearrangement to the higher energy **30** under the conditions utilized in the experiment.

Acknowledgment. One of us (J. I. M.) acknowledges the support of the National Science Foundation and the Office of Naval Research.

(27) A. C. Logothetis, G. N. Gausen, and R. J. Shozdy, *Inorg. Chem.*, 2, 173 (1963).

Localized Molecular Orbitals and Chemical Reactions. II. A Study of Three-Center Bond Formation in the Borane–Diborane Reaction

David A. Dixon, Irene M. Pepperberg, and William N. Lipscomb*

Contribution from the Gibbs Chemical Laboratory, Harvard University, Cambridge, Massachusetts 02138. *Received September 21, 1973*

Abstract: Comparison of the symmetric (C_{2h}) approach of two BH_3 molecules to form B_2H_6 with the unsymmetric (C_s) approach in which only a single hydrogen bridge is formed leads to strong preference for the C_{2h} transition state having two very unsymmetrical hydrogen bridges. This symmetric state lies 2.6 kcal/mol of B_2H_6 higher than $2BH_3$ in a self-consistent field calculation extended by inclusion of all 14 single and 210 double excitations from the valence shells of a minimum Slater basis. The two equivalent unsymmetrical bridges have a long B···H interaction with a B–B distance of 3.0 Å in the transition state. The formation of the three-center BH_bB bond is investigated by examining the properties of the localized molecular orbitals along the symmetric pathway. A covalent three-center (bent) B–H···B forms as the B···B distance closes to about 2.1 Å, corresponding to a H···B distance of 1.65 Å.

The diborane molecule has been the object of much theoretical work[1] since it is the prototype boron hydride. The dimerization of two boranes to form diborane

$$2BH_3 \rightleftharpoons B_2H_6 \qquad (1)$$

is the simplest reaction involving the formation of B–H–B three-center bonds from B–H two-center terminal bonds. The small size of the molecules involved in reaction 1 and the considerable theoretical work done on the system[2] make it attractive for a theoretical study of the reaction pathway. The reverse of reaction 1, which we shall call 1b, is of substantial experimental importance[3–8] as the generally accepted first step in the diborane pyrolysis (except for the proposal of Long[8]). Most of the higher boranes are generated *via* a chain mechanism from the initial decomposition of diborane (reaction 1b).

(1) E. A. Laws, R. M. Stevens, and W. N. Lipscomb, *J. Amer. Chem. Soc.*, **94**, 4461 (1972), and references therein.

(2) (a) J. H. Hall, Jr., D. S. Marynick, and W. N. Lipscomb, *Inorg. Chem.*, **11**, 3126 (1972); (b) M. Gehlus, R. Ahlrichs, V. Staemmler, and W. Kutzelnigg, *Chem. Phys. Lett.*, **7**, 503 (1970); (c) C. Edmiston and P. Lindner, *Int. J. Quantum Chem.*, **7**, 309 (1973).

(3) R. P. Clarke and R. N. Pease, *J. Amer. Chem. Soc.*, **73**, 2132 (1951).

(4) J. K. Bragg, L. V. McCarty, and F. J. Norton, *J. Amer. Chem. Soc.*, **73**, 2134 (1951).

(5) R. Schaeffer, as quoted in "Production of the Boranes and Related Research," R. T. Holzmann, Ed., Academic Press, New York, N. Y., 1967, p 121.

(6) W. N. Lipscomb, "Boron Hydrides," W. A. Benjamin, New York, N. Y., 1963, p 177.

(7) R. Schaeffer, *J. Inorg. Nucl. Chem.*, **15**, 190 (1960).

(8) L. H. Long, *J. Inorg. Nucl. Chem.*, **32**, 1097 (1970).

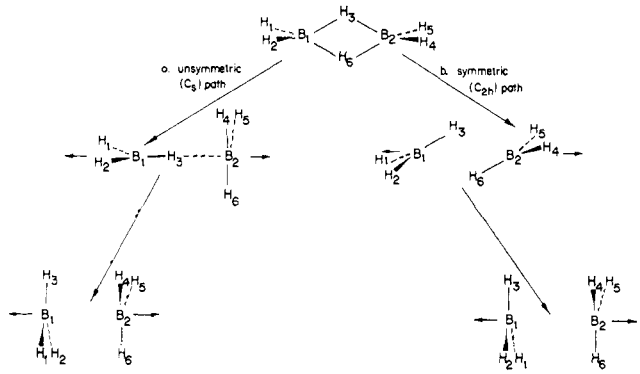

Figure 1. Postulated reaction pathways for $B_2H_6 \rightleftarrows 2BH_3$.

In an earlier note[2a] the presumed near-Hartree–Fock limit of −19 kcal/mol of B_2H_6 has been found for the ΔE of reaction 1b. The correlation correction, not yet calculated and probably large due to the formation of three-center bonds, will surely correct this value toward the recent experimental value of −34.9 kcal/mol, which corresponds to a ΔH of −35.5 kcal/mol. In a recent experimental study, Mappes, Fridmann, and Fehlner studied the borane recombination reaction and found an activation energy for reaction 1b of 0 ± 2 kcal/mol.[9] They also proposed a transition state with a single BHB bridge (Figure 1) for the recombination. In ref 2a we first proposed a transition state with two symmetrically equivalent BHB bridges (Figure 1). Recently, Gimarc[10] has published an extended Hückel (EHT) calculation for these two pathways and compares them using correlation diagrams. However, at the EHT level of sophistication, a preference for one of these two pathways cannot be made. All of the results described below are obtained with a minimum Slater basis from the SCF method[11,12] corrected in many instances by configuration interaction, or obtained with a new and efficient approximation to the SCF method called partial retention of diatomic differential overlap (PRDDO).[13,14]

We compare theoretical energies calculated by the three methods mentioned above for the two proposed pathways and find the symmetric C_{2h} (double bridge) pathway to be energetically more favorable. We preclude, however, a discussion of the free-energy surface as we have not included an entropy effect. For this pathway we investigate localized molecular orbitals[15] obtained from the SCF wave function at various points on the pathway in order to investigate bonding in the transition-state region and to investigate the formation of the covalent three-center BHB bonds.

Calculations

The three methods of calculation, PRDDO, SCF, and SCFCI, increase in sophistication and accuracy in this order. Since the SCF and SCFCI methods have been discussed in great detail and are familiar, we do not describe them. However, due to the recent introduction of PRDDO we now describe this method briefly.

PRDDO is a nonempirical SCF method for studying electronic structure, originally developed to study large molecules at a reasonable level of sophistication with minimal cost. The major points of the method follow.

(1) The original minimum basis set of atomic orbitals is Löwdin orthogonalized to a new basis set. It is found that three- and four-center exchange integrals are small in this basis and can be neglected. Thus, the basis set transformation allows us to pass the physical content of N^4 integrals, where N is the number of atomic orbitals, to N^3 integrals. We note here that the Löwdin transformation allows the closest correspondence of the new basis to the original atomic orbital basis.

(2) By defining nonspherical orbital components in terms of local spherical axes, there is no need to use single center averaging to preserve rotational invariance. Thus, all kinetic energy, overlap, and nuclear attraction integrals are accurately calculated over Slater type orbitals and are then transformed to the new basis set.

(3) All one-center Coulomb and exchange integrals in the Löwdin basis are evaluated approximately as are the two- and three-center electron repulsion Coulomb integrals. Due to the basis set transformation, a unique nuclear center does not exist for each orbital and, therefore, analytical expressions for the integrals are not available. The major approximation in the calculation of these integrals is the use of spherical charge densities for the charge distribution $\varphi_k(2)^2$ in integrals of the form $(\varphi_i(1)\varphi_j(1)|\varphi_k^2(2))$.

(4) Exchange integrals of the forms $(i_A j_A | i_A j_A)$ and $(i_A j_B | i_A j_B)$ for centers A and B are retained and are approximated as described above in (3).

Two versions of the method are described in the literature. We use the parameterized version, since it is more accurate than the unparameterized method. The parameterization is obtained by least-squares fitting the two-electron G matrix elements calculated by the unparameterized PRDDO version with a large number of minimum basis set SCF calculations. We emphasize that it is still a nonempirical method as the parameters are chosen from *ab initio* results in contrast with the empirical parameters used in the other common approximate methods, CNDO and INDO.[16]

The SCF wave function, eigenvalues, and energies were obtained from Stevens' program.[17] The configuration interaction addition[18] to this program was applied to all single and double excitations from the valence electrons only to all virtual orbitals. Programs, also from this laboratory, were used for further analysis of results and for conversion of molecular orbitals to localized orbitals[15] by the Edmiston–Ruedenberg procedure.[19] The parameterized PRDDO program was written by Halgren.[13,14] All computations were carried out on an IBM 360/91. Computational times for each geometry were 2.3 sec for PRDDO, 55 sec for SCF, and 25 sec for localizations.

(9) G. W. Mappes, S. A. Fridmann, and T. P. Fehlner, *J. Phys. Chem.*, **74**, 3307 (1970).
(10) B. M. Gimarc, *J. Amer. Chem. Soc.*, **95**, 1417 (1973).
(11) C. C. J. Roothaan, *Rev. Mod. Phys.*, **23**, 69 (1951).
(12) G. G. Hall, *Proc. Roy. Soc., Ser. A*, **205**, 541 (1951).
(13) T. A. Halgren and W. N. Lipscomb, *Proc. Nat. Acad. Sci. U. S.*, **69**, 652 (1972).
(14) T. A. Halgren and W. N. Lipscomb, *J. Chem. Phys.*, **58**, 1569 (1973).
(15) (a) E. Switkes, R. M. Stevens, W. N. Lipscomb, and M. D. Newton, *J. Chem. Phys.*, **51**, 2085 (1969); (b) E. Switkes, W. N. Lipscomb, and M. D. Newton, *J. Amer. Chem. Soc.*, **92**, 3847 (1970); (c) M. D. Newton, E. Switkes, and W. N. Lipscomb, *J. Chem. Phys.*, **53**, 2645 (1970); (d) M. D. Newton and E. Switkes, *ibid.*, **54**, 3179 (1971).
(16) J. A. Pople and D. L. Beveridge, "Approximate Molecular Orbital Theory," McGraw-Hill, New York, N. Y., 1970.
(17) R. M. Stevens, *J. Chem. Phys.*, **52**, 1397 (1970).
(18) K. Morokuma and H. Konishi, *J. Chem. Phys.*, **55**, 402 (1971).
(19) C. Edmiston and K. Ruedenberg, *Rev. Mod. Phys.*, **35**, 457 (1963).

A minimum Slater basis was used throughout with previously optimized exponents for BH_3[20] and B_2H_6.[15a] Transition-state exponents were constructed from a weighted average of B_2H_6 terminal and bridge exponents as given in Table I. The difference in total energy using

Table I. Exponents for Slater Orbitals

	BH_3[a]	B_2H_6[b]	B_2H_6TS[c]
B (1s)	4.6838	4.68	4.68
(2s)	1.4489	1.4426	1.4426
(2p)	1.4836	1.4772	1.4772
H (1s)	1.136		
H_t (1s)		1.1473	1.168
H_b (1s)		1.2095	1.168

[a] Reference 20. [b] Reference 15a. [c] Boron exponents: ref 15a. H exponents: weighted average of H_t and H_b exponents (footnote *b*); $(2H_b + 4H_t)/6 = 1.168$.

the two sets of exponents for B_2H_6 is only 1 kcal/mol. Starting geometries were the calculated optimized D_{3h} structure for BH_3[2] and the experimental structure for B_2H_6.[21]

Optimized geometries were obtained, using these exponents, for BH_3, B_2H_6, and various intermediate geometries for two reaction pathways: first, the previously suggested[9] initial formation of an unsymmetrical single bridge hydrogen (Figure 1a), and second, the initial formation of two equivalent but unsymmetrical bridge hydrogens (Figure 1b). We shall refer to these respectively as the unsymmetrical (C_s) (Figure 1a) and the symmetrical (C_{2h}, Figure 1b) paths and transition states (TS). Geometry optimization for structures along the reaction pathway was first carried out by the PRDDO method, and these geometries were further optimized by the SCF method and a small number were checked by the SCF–CI method. A comparison of the results for optimized SCF and PRDDO calculations at a point on the pathway gives good agreement for geometries; the B–H_t distances given by the PRDDO calculations are shorter by 0.02 Å for BH_3 and 0.035 Å for B_2H_6, but B–H_b distances agree to within 0.01 Å, and bond angles agree to within 2°. In agreement with the results of Halgren and Lipscomb,[13,14] who found E(SCF) − E(PRDDO) = 0.03 au for B_2H_6, we find for the transition-state calculations that the PRDDO total energies are uniformly approximately 0.03 au more negative than the SCF results. Thus, both geometries and relative energies at all B–B distances along the C_{2h} pathway are accurately reproduced by PRDDO in comparison with SCF rseults.

Energies and Pathway

Optimized geometries of B_2H_6, BH_3, and the symmetric path (Figure 1b) are shown in Table II for both the PRDDO and SCF method. Results for the previously suggested unsymmetric path[9] (Figure 1a) are given in Table IV.

Reaction Energy. Total energies (Table III) yield 7.3 kcal/mol for the SCF dissociation energy of B_2H_6 into $2BH_3$ and an additional 9.3 kcal/mol for the correction due to single and double excitations from the

(20) E. Switkes, R. M. Stevens, and W. N. Lipscomb, *J. Chem. Phys.*, **51**, 5229 (1969).

(21) L. S. Bartell and B. L. Carroll, *J. Chem. Phys.*, **42**, 1135 (1965).

Table II. Geometry Optimization[a] (Comparison between PRDDO and SCF Methods for B_2H_6, BH_3, and the Symmetrical (C_{2h}) Transition State)

B–B dist:	3.354		3.774		3.98		4.334		4.612		5.031		5.451		5.872		BH_3[f]	
Method:	PRDDO[b]	SCF[b]	PRDDO	SCF	PRDDO	SCF	PRDDO	SCF	PRDDO	SCF	PRDDO	SCF	PRDDO	SCF	PRDDO	SCF	PRDDO[b]	SCF[b]
BH_t	2.192	2.260	2.19	2.25	2.19	2.25	2.19	2.23	2.23	2.23	2.19	2.23	2.19	2.23	2.19	2.23	2.21	2.25
BH_b	2.530	2.530	2.48	2.49	2.36	2.37	2.23	2.28	2.22	2.27	2.20	2.25	2.20	2.24	2.20	2.24	—	—
B_1–H_3–B_2	83.02°	83.02°	90.92°	90.83°	92.23°	92.04°	92.58°	92.82°	93.81°	95.16°	95.72°	96.11°	96.89°	97.53°	102.07°	100.48°	—	—
H_3–B_2–H_6	97.97°	96.97°	89.07°	89.17°	87.77°	87.96°	87.42°	87.18°	86.19°	84.84°	84.28°	83.89°	83.11°	82.47°	77.93°	79.52°	—	—
H_1–B_1–H_2	120.97°	119.00°	—	—	—	—	—	—	—	—	—	—	—	—	—	—	—	—
H_1–B_1–H_3	109.05°	109.65°	113.34°	113.34°	116.41°	116.41°	118.63°	118.76°	119.07°	119.26°	119.20°	119.49°	119.47°	119.52°	119.50°	119.57°	(120°)	(120°)
H_1–B_1–B_2[c]	180.00°	180.00°	170.00°	170.00°	144.00°	144.00°	137.00°	137.00°	132.00°	132.00°	125.0°	125.0°	123.0°	122°	124°	122°	—	—
H_3–B_1–B_2	48.98°	48.48°	47.99°	47.99°	51.49°	51.49°	56.5°	55.5°	57.5°	56.0°	58.5°	57.5°	59.5°	58.5°	59.5°	58.5°	—	—

[a] All distances are in au. [b] Geometry obtained by optimization. [c] For all geometries, H_1–B_1–B_2 represents the angle between the BH_t plane and the B–B axis. [d] Values in parentheses were not varied in optimization. [e] All unlisted angles are assumed to be the same as those in B_2H_6 (double dash). [f] Not necessary (single dash). The reader should note that the B–B distance of 3.354 is that of B_2H_6.

Table III. Total Energies (au) for Symmetric (C_{2h}) and Unsymmetric (C_s) Pathways

	B_2H_6	C_{2h}	C_s	C_{2h}	C_s	C_{2h}	C_s	C_{2h}	C_s	C_{2h}	C_s	C_{2h}	C_s	$2BH_3$ (∞)
B–B distance	3.3543	3.7736	3.9849	4.3345	4.1929	4.6122		5.0315	5.031	5.450	5.451	5.872	5.872	
PRDDO	−52.7483	−52.7392		−52.7329		−52.7308	−52.6488	−52.7318		−52.7337	−52.7154	−52.7349	−52.7274	−52.7353	−52.7333	−52.7366[a]	−52.7444[b]
SCF	−52.7183	−52.7119		−52.7058		−52.7027		−52.7024		−52.7031		−52.7038	−52.6954	−52.7043	−52.7004	−52.7066[b]	
SCF–CI	−52.8298	−52.8244		−52.8139		−52.8033		−52.8010		−52.7997		−52.7991	−52.7922	−52.7992	−52.7967	−52.8032[b]	

[a] Weighted averaged exponents were used (footnote *c*, Table I). [b] SCF exponents, ref 15a.

Table IV. Geometry Optimizations[a] for the Unsymmetrical (C_s) Transition State

B–B dist:	5.872		5.451		5.031	4.193
Method:	PRDDO	SCF	PRDDO	SCF	PRDDO	PRDDO
BH_t	2.192	2.240	2.192	2.240	2.192	2.192
B_1–H_1	2.180	2.230	2.175	2.195	2.130	1.970
B_2–H_1	3.692	3.642	3.276	3.256	2.901	2.223

[a] All distances are in au.

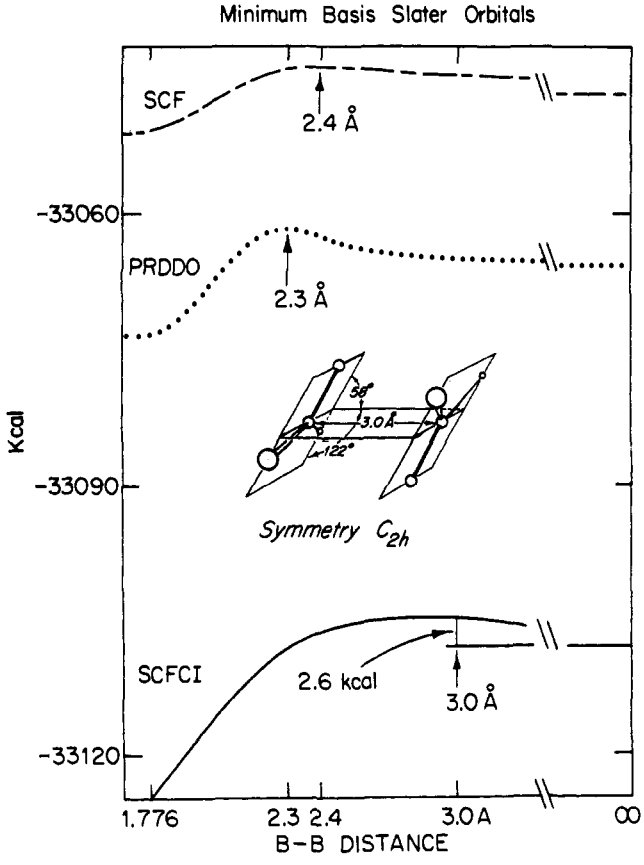

Figure 2. Energy profiles along the symmetric (C_{2h}) reaction pathways for the three types of calculation: PRDDO, SCF, and SCF–CI. Units for the abscissa are in kilocalories per mole.

valence shell of the minimum Slater set of atomic orbitals. Thus, the minimum basis set results corrected by CI yield a ΔE of -17 kcal/mol for

$$2BH_3 \longrightarrow B_2H_6$$

Comparison of these results with those of the near-Hartree–Fock calculation[2a] (-19 kcal/mol) and the most probable experimental value -35 kcal/mol[9] shows that we have obtained approximately one-half of the Hartree–Fock reaction energy and one-half of the correlation energy difference. These results emphasize the point that SCF results and configuration interaction corrections from different basis sets should not be added together. Our ΔE of -17 kcal/mol for the reaction energy is quite far from the experimental results, and this difficulty should be remembered in viewing our discussion of the activation energy.

Pathway Choice. A comparison of total energies for the symmetric (C_{2h}) and unsymmetric (C_s) pathways (Table V) at the PRDDO level of approximation indicates that the unsymmetric pathway is always less stable at any given B···B distance. In the transition-state region for the SCF–CI calculation, SCF and SCFCI

Table V. Activation Energies for the Symmetric (C_{2h}) Pathways

	Activation energies, C_{2h}TS, kcal/mol	
	a	*b*
PRDDO	3.6	8.6
SCF	2.6	
SCF–CI	2.6	

[a] Weighted averaged exponents were used (footnote *c*, Table I). [b] SCF exponents, ref 15a.

energies for the two pathways were calculated; here the C_{2h} pathway was lower in energy although only by about 2 kcal/mol. However, an attempt to optimize the C_s pathway structure at a fixed B···B distance yielded the C_{2h} pathway structure at that distance. This result strengthens our conclusion that the symmetric transition state is to be preferred, since the energy differences alone are too small to distinguish the correct pathway at the minimum basis set level. We would like to emphasize at this point that we have chosen the two most chemically reasonable geometries for the approach but that this study represents only a small part of the complex multidimensional potential energy surface. Indeed, all such theoretical investigations of surfaces for complex chemical reactions, especially for polyatomic systems,[22] must be viewed in this light since a complete study of the total surface is usually prohibitively costly.

Symmetrical Pathway. The activation energy, *i.e.*, the energy of the C_{2h} transition state over that for $2BH_3$, is about 2.5 kcal/mol in the SCF–CI approximation (Table V). Because of the incompleteness of the basis set, this activation energy is probably an upper bound as indicated by basis extension, which stabilizes B_2H_6 relative to $2BH_3$. The experimental value[9] is uncertain but is small (0 ± 2 kcal/mol) and therefore not in disagreement with our theoretical result. An energy analysis for this symmetric pathway is shown in Table VI.

As a function of B···B distance (Figure 2), the energy profiles of the symmetric (C_{2h}) approach show maxima at different B···B distances for the PRDDO, SCF, and SCF–CI methods. Most interesting is the broadening and displacement of the energy–coordinate curve for the best of these three calculations, the SCF–CI result. The need for the CI contribution is quite clear at this minimum basis level, but of course this need will have to be reevaluated if and when larger basis sets can be employed. O'Neil, Pearson, Schaeffer, and Bender[23] have noted a similar broadening of the transition state by CI in their study of the H + F_2 surface. They found an increase of 0.5 Å in the HF distance at the transition state when comparing SCF–CI with SCF for a double ζ

(22) D. M. Silver and R. M. Stevens, *J. Chem. Phys.*, **59**, 3378 (1973), discuss the problems of geometrical degrees of freedom for the H_2 + H_2 reaction.

(23) S. V. O'Neil, P. K. Pearson, H. F. Schaefer, III, and C. F. Bender, *J. Chem. Phys.*, **58**, 1126 (1973).

Table VI. SCF Energetics[a] (au) for Symmetric (C_{2h}) Approach

B–B distance	Nuclear repulsion energy	Nuclear attraction energy	Kinetic energy	Two-electron energy	Coulomb energy[b]	Exchange energy[c]	Self-repulsion energy[d]	SCF energy	$-E/T$
3.354[e]	31.7483	−183.9020	52.6271	46.8087	51.2443	−4.4356	5.4318	−52.7183	1.0017
3.774	30.3027	−181.1153	52.5960	45.5048	50.0164	−4.5116	5.3346	−52.7119	1.0022
3.985	29.6478	−179.9472	52.6697	44.9259	49.5073	−4.5814	5.2777	−52.7058	1.0007
4.334	28.8141	−178.5003	52.8058	44.1776	48.8782	−4.7006	5.1930	−52.7027	0.9981
4.612	28.1285	−177.2141	52.8291	43.5541	48.3135	−4.7594	5.1398	−52.7024	0.9976
5.031	27.1475	−175.3398	52.8466	42.6437	47.4852	−4.8415	5.0629	−52.7031	0.9973
5.451	26.3110	−173.7112	52.8559	41.8399	46.7448	−4.9048	5.0029	−52.7038	0.9971
5.870	25.5665	−172.2410	52.8535	41.1178	46.0699	−4.9521	4.9558	−52.7043	0.9972
f	14.8729	−150.6909	52.7143	30.3972	31.6890	−1.2919	8.5716	−52.7066	0.9999

[a] 1 au of energy is 627.5 kcal/mol. [b] $\Sigma_{i>j} 4(ii|jj)$. [c] $-\Sigma_{i>j} 2(ij|ij)$. [d] $\Sigma_i (ii|ii)$. [e] B_2H_6. [f] Results for $2BH_3$.

basis set. We note that their surface is similar to ours in that a low activation energy (1.0 kcal/mol for $H + F_2$) and a broad transition-state region are present. We also point out that a "good" activation energy may not be the best criterion for choosing a theoretical transition state, as revealed by a comparison of either the PRDDO or the SCF results with the SCF–CI results (Table V). The activation energies are close to each other and in good agreement with experiment. However, the B–B distance in the transition state differs substantially between the PRDDO or SCF results and the SCF–CI results. Thus, an incorrect distance in the transition state with "good" energy was obtained in the absence of the CI correction. We note also that the B···B distances in the SCF and PRDDO transition states differ by only 0.1 Å.

From the energy and geometry changes alone, a qualitative description of the C_{2h} symmetric pathway can be obtained. As the borane molecules approach one another along the C_{2h} pathway, each tilts away from the BB axis in such a way that *one* of its hydrogens moves toward the opposite boron; the two boranes remain parallel and appear to move in a concerted fashion. At a B···B distance of 4.33 au, the borane molecules have become quite nonplanar, and formation of the two BHB three-center bonds has begun (see below). The two molecules are now more stable in a B_2H_6-type configuration rather than in a configuration resembling two BH_3 molecules. Hence, the terminal hydrogens swing toward the B–B axis to give tetrahedral bonding at each boron rather than the planar trigonal bonding found in borane.

At B···B distances of less than 4.33 au, the bridge hydrogen position is well fixed with regard to the H_b–B–B angle and B–H_b (parent boron) distance. The major geometry change along this portion of the reaction pathway involves the rotation of the terminal hydrogens toward the molecular plane containing borons and terminal hydrogens in B_2H_6, finally resulting in the perpendicular planes of the bridge and terminal hydrogens found in diborane. We also note that the change in hybridization in going from trigonal to tetrahedral is energetically favorable.

Configuration interaction results (Table VII and Figure 3) show that this correction increases the B···B distance in the transition state. As diborane dissociates, the CI correction which partially acounts for the correlation energy should decrease in absolute value (become more positive) due to the decrease in the number of pairs that can interact. At a B···B separation distance of infinity this energy in the Hartree–Fock CI limit should correspond to twice the correlation energy of two boranes. The CI energy curve is shown in Figure 3, and as diborane dissociates the CI energy correction approaches an asymptotic limit. However, the asymptotic limit appears to be greater than that of two boranes, suggesting possibly that BH_3 is better defined by the minimum basis set and CI correction than is the B_2H_6 transition-state region. Thus, it is likely that an extended basis set study with CI corrections would lead to little or no activation barrier for the reaction. In order to account for other possibilities, the single excitations were excluded producing only a slight change in the CI energy; exponents from BH_3 for boron and all hydrogens were used, resulting in a very small CI energy change (Table VII). An increase of 1 au in the B···B distance to 6.87 au increased the CI energy slightly in accord with the probable result that the calculation goes to an asymptotic unit. Thus if the two cal-

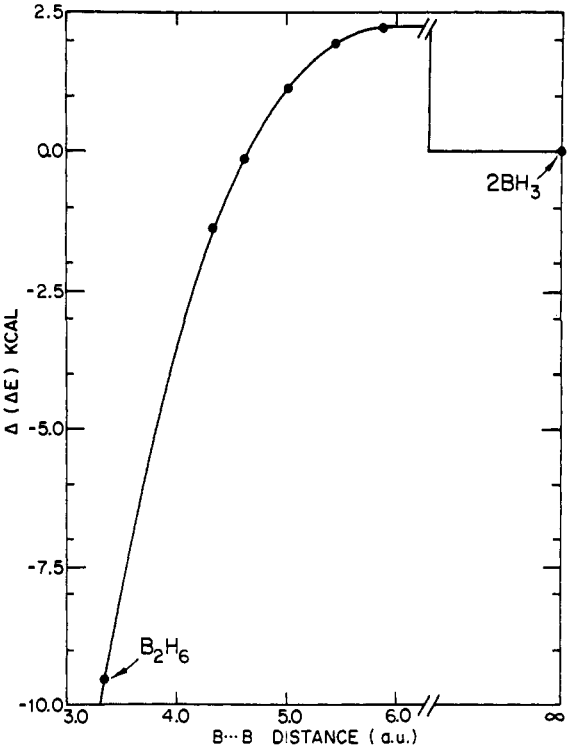

Figure 3. Plot for configuration interaction changes as a function of B···B distance for the symmetric pathway. Values of E are E(SCF–CI) − E(SCF). From each ΔE we subtract $2\Delta E$ for BH_3 to find $\Delta(\Delta E)$. Units for the abscissa are in kilocalories per mole.

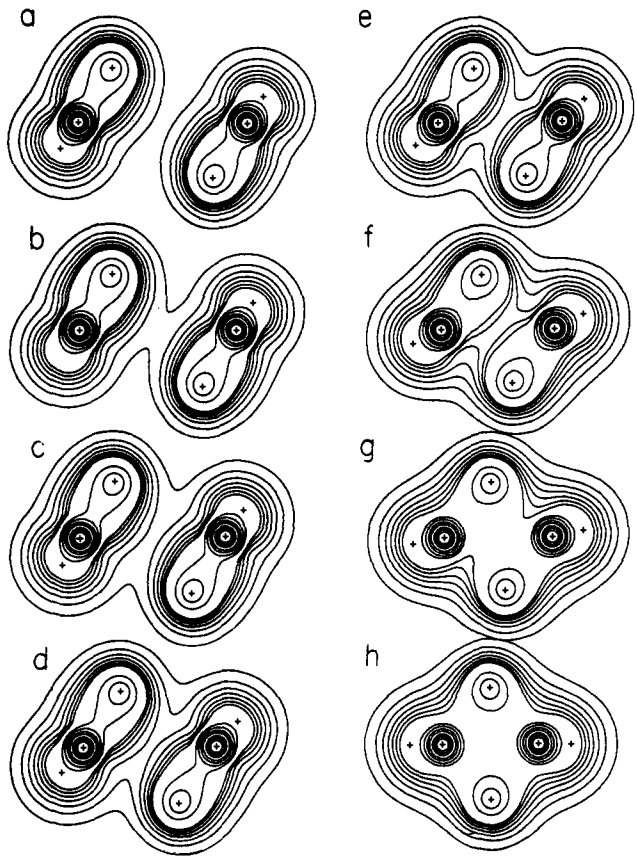

Figure 4. Total electron density maps for the symmetric pathway for the various B–B distances: (a) 5.87; (b) 5.45; (c) 5.03; (d) 4.61; (e) 4.33; (f) 3.98; (g) 3.77; (h) 3.54 au (diborane). Contour levels (e/au^3) are 10.0, 5.0, 2.5, 1.0, 0.5, 0.25, 0.15, 0.07, 0.06, 0.05, 0.04, 0.03, 0.02, and 0.01. The "+" marks are the atomic positions and are labeled in Figure 5a for clarity with H and B.

culations had the same asymptotic limit, the continuous increase in the CI energy as diborane is formed would cancel the activation energy barrier of the SCF calculation. This conclusion is consistent with the lengthening of the B···B distance in the SCF–CI transition state compared to that of the SCF transition state. As the BB distance decreases past the transition state, the CI correction increases, stabilizing formation of B_2H_6 with respect to re-forming two boranes. Thus, the energy along the pathway falls off as shown in Figure 2. This effect as the B···B distance decreases is expected since diborane is stabilized by 9.3 kcal/mol with respect to two boranes. A much smaller effect is the very slightly greater magnitude of the configuration interaction correction for the C_s transition state as compared with the C_{2h} transition state when compared at the same B···B distance in the range from 5.45 to 5.87 au (Table VII). This effect is probably due to the somewhat better overlap between H and the vacant orbital on B in the direct approach in the C_s geometry; a more stable three-center bond is found. Nevertheless, the C_s geometry still gives an unfavorable total energy at all B···B distances.

Finally, variation of the hydrogen exponent, followed by geometry optimization at a B···B distance of 5.45 au for the C_{2h} model, resulted in no change in the SCF–CI activation energy. The effect of triple and quadruple excitations from the valence shell changed the configuration interaction correction energy of BH_3 from −31 to −32 kcal/mol. This change is comparable with that (4%) noted earlier for the Be atom[24] which was an extended basis set calculation with many configurations. Since we are taking differences, we feel that these additional excitations would probably change the parameters for a reaction by an even smaller percentage.

Table VII. Configuration Interaction (SCF–CI) Energy Results (au)

Molecule	No. of determinants	No. of eigenvectors
$BH_3(C_{2v})^a$	67	35
$BH_3(C_{2v})^b$	279	130
$B_2H_6(C_{2h})^c$	841	335
$B_2H_6(C_s)$	1657	645

	A = E(SCF–CI) − E(SCF)	E(SCF–CI)
BH_3 $(C_{2v})^i$	−0.0483	−26.4016
BH_3 $(C_{2v})^a$	−0.0492	−26.4015
BH_3 $(C_{2v})^{b,i}$	−0.0496	−26.4029
B_2H_6 (C_s) (5.87 au)^d	−0.0962	−52.7967
B_2H_6 (C_s) (5.45 au)^d	−0.0968	−52.7922
B_2H_6 (C_{2h}) (5.87 au)^d	−0.0949	−52.7992
B_2H_6 (C_{2h}) (5.45 au)^d	−0.0953	−52.7991
B_2H_6 (C_{2h}) (5.03 au)^e	−0.0966	−52.7997
B_2H_6 (C_{2h}) (4.61 au)^e	−0.0986	−52.8010
B_2H_6 (C_{2h}) (4.33 au)^e	−0.1006	−52.8033
B_2H_6 (C_{2h}) (3.98 au)^e	−0.1082	−52.8139
B_2H_6 (C_{2h}) (3.77 au)^e	−0.1125	−52.8244
B_2H_6 (C_{2h}) (5.45 au)^e	−0.0955	−52.7985
B_2H_6 (C_{2h}) (5.45 au)^e	−0.0953	−52.7978
B_2H_6 (C_{2h}) (5.45 au)^f	−0.0946	−52.7991
B_2H_6 (C_{2h}) (5.87 au)^f	−0.0941	−52.7992
B_2H_6 $(C_{2h})^g$	−0.1132	−52.8298
B_2H_6 $(C_{2h})^h$	−0.1136	−52.8318
B_2H_6 (C_{2h}) (5.87 au)^i	−0.0934	−52.7991 (SCF = −52.7057)
B_2H_6 (C_{2h}) (5.87 au)^j	−0.0932	−52.7989 (SCF = −52.7057)
B_2H_6 $(C_2)_h$ (6.87 au)^k	−0.0930	−52.7990 (SCF = −52.7061)

[a] All single and double excitations from the valence shell were included. The geometry of BH_3 is D_{3h}, but the computation was carried out in the subgroup C_{2v} (weighted averaged exponents used). [b] All single, double, triple, and quadruple excitations from the valence shell were included. Again the C_{2v} subgroup of D_{3h} was used. [c] Symmetric approach. [d] Unsymmetric approach. [e] This is a geometry check. Bridge hydrogen coordinates were changed. Thus, the CI energy at these large distances does not show a critical dependence on the exact geometry. [f] This is an exponent check. We changed the hydrogen exponents to an intermediate value between those for borane and diborane. Thus, the CI energy does not critically depend on having exact exponents. [g] Weighted averaged exponents were used. [h] SCF optimized exponents were used. [i] BH_3 optimized exponents were used. [j] Same exponents as *i*. Skip single excitations. [k] Same exponents as *i*. Increase B···B distance with no geometry optimization.

Localized Orbitals

The total electron density (Figure 4) and total energy

(24) C. F. Bunge, *Phys. Rev.*, **168**, 92 (1968).

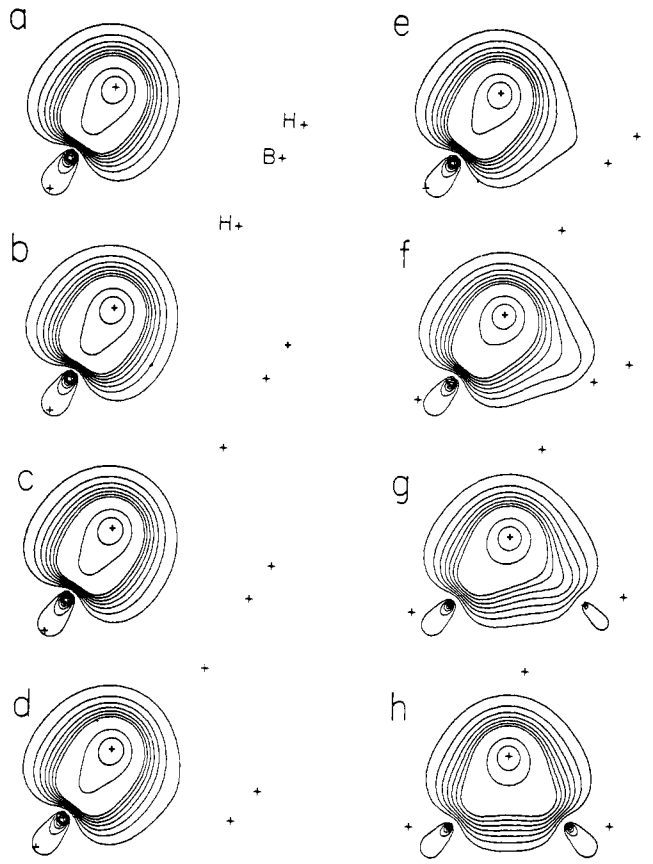

Figure 5. Electron density maps for a localized B–H bond that becomes the BH_bB bond in diborane as seen along the symmetric pathway. Distances, contour levels, and atomic positions as in Figure 4.

are, of course, invariant[11,25] under the kind of unitary transformations which convert symmetry orbitals, or some other starting set of molecular orbitals, into localized molecular orbitals. Following an earlier study[26] of the behavior of rigorously derived localized orbitals in a chemical reaction, we present here a similar analysis of localized orbitals in the dimerization of $2BH_3$ to give B_2H_6. We would like to emphasize that this localization was done on only the symmetric path with the minimum basis integrals and wave function. The localized orbitals for which electron densities for the bridge orbital (two electrons per orbital) are shown in Figure 5 were derived by maximizing the self-repulsion energy (Table VIII), which gives a corresponding minimization of the exchange energy and the *inter*-orbital Coulombic energy as seen by comparing Tables VI and VIII.

Total electron density plots (Figure 4), electron density plots of the bridge LMO (Figure 5), and wave function plots of the bridge LMO (Figure 6) yield a wealth of information. When coupled with a population analysis of the LMO's into atomic orbital components, a reasonable description of the covalent formation of the three-center bond is provided. As the molecules approach, a slight increase in B···B midpoint density (Figures 4a and 4b) between 5.87 and 5.45 au occurs without noticeable distortion of the BH bonds of the slightly deformed BH_3 units. Only when the B···B distance falls to

(25) V. Fock, *Z. Phys.*, **61**, 126 (1930).
(26) D. A. Dixon and W. N. Lipscomb, *J. Amer. Chem. Soc.*, **95**, 2853 (1973).

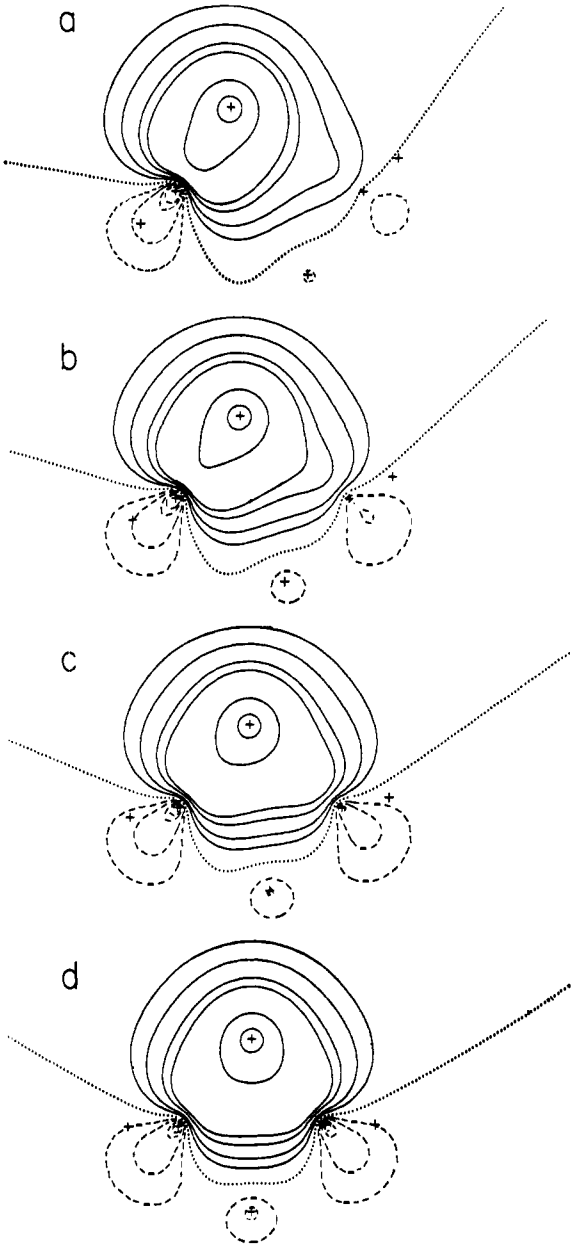

Figure 6. Plots of the wave function of the localized three-center bond in diborane and at the three shortest dissociation points. B–B distances are (a) 4.33; (b) 3.98; (c) 3.77; (d) 3.54 au (diborane). Contour levels (e/au^3) are with solid lines corresponding to positive phase, dashed lines to negative phase, and the dotted line is the nodal line (magnitude of $\varphi = 0$). The "+" marks correspond to atomic positions as labeled in Figure 5.

Table VIII. Localization Energetics (au)

B–B distance, au	Coulomb[a] energy	Exchange[b] energy	Self-repulsion[c] energy
3.354[d]	47.0773	−0.2685	9.5788
3.774	45.7515	−0.2467	9.5996
3.985	45.1587	−0.2328	9.6263
4.334	44.3938	−0.2162	9.6773
4.612	43.7626	−0.2085	9.6907
5.031	42.8441	−0.2004	9.7040
5.451	42.0364	−0.1965	9.7113
5.872	41.3122	−0.1944	9.7135
e	30.5862	−0.1890	9.6745

[a] $\Sigma_{i>j} 4(ii|jj)$. [b] $\Sigma_{i>j} 2(ij|ij)$. [c] $\Sigma_i (ii|ii)$. [d] The 3.354 distance is that in B_2H_6 itself. [e] Results are given for $2BH_3$.

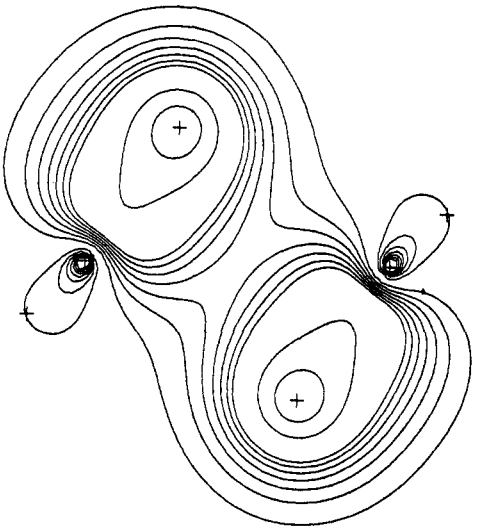

Figure 7. Electron density map for the combined localized B–H_b–B orbitals at a B–B distance of 4.33 au showing the density along the B···B axis. Contours and "+" marks are those of Figure 4.

about 4.61 au (Figure 4d) do we find slight BH bond distortions; these become quite noticeable at about 4.33 au (Figure 5e). These distortions give rise to the density of the two BH_bB bridge bonds, which account for most of the B···B midpoint density at these shorter distances (Figure 7). Thus, in the SCF transition-state region very little electron rearrangement occurs.

It is only as the B···B distance approaches the distance in diborane that the formation of the three-center bond can be investigated. At 3.98 au the total electron density still resembles total densities at larger B···B distances (Figure 4f). However, at 3.77 au (Figure 4g) the total density is more like that of B_2H_6 (Figure 4h) with the absence of an electron density valley between the two borons. In B_2H_6 the bridge hydrogen density tends toward the molecular center while, as the two boranes approach, the density of the bridge hydrogen is directed toward the parent boron. It is only at 4.33 au that any distortion in the bridge hydrogen orbitals (Figure 5g) toward the center is noticeable, but the distortion is at a level where it is not yet seen in the total density map. The B–H_b–B orbital plot at 3.98 au (Figure 5f and Table IX) shows a strongly perturbed B–H_b bond corresponding to the beginning of electron reorganization in the molecule. At 3.77 au the B–H_b–B plot (Figure 5g) shows a node at the far boron with the result that the three-center bond closely resembles that in B_2H_6.

The plots of the LMO bridge wave function (Figure 6) clarify the nodal structure of the system and give a more reliable measure of the distance where the three-center bond is formed. With the exception of the distorted hydrogen orbital the plot at a B···B distance of 3.77 au (Figure 6c) closely resembles that of B_2H_6 (Figure 6d), showing an identical nodal structure and a similar density on the B–B axis. At 3.98 au (Figure 6b) there is little distortion of the hydrogen orbital from that present in BH_3, but the density along the BB axis is essentially that in B_2H_6. However, the nodal structure has changed radically, especially in the region of the far boron, and is very similar to the nodal structure at 4.33 au (Figure 6a). At 4.33 au very little bonding is evident as seen by the unperturbed inner contours.

Table IX. Population Analysis of Localized Orbitals Symmetric Pathway

B–B distance		Inner shell	B–H_t	BH_bB
3.354[a]	B	2.003	0.934	0.506
	H_t		1.085	
	H_b			1.016
3.774	B	2.003	0.946	0.575 (0.344)[b]
	H_t		1.070	
	H_b			1.117
3.986	B	2.003	0.941	0.709 (0.202)[b]
	H_t		1.075	
	H_b			1.111
4.334	B	2.003	0.935	0.825
	H_t		1.082	
	H_b			1.112
4.612	B	2.003	0.931	0.855
	H_t		1.085	
	H_b			1.115
5.031	B	2.003	0.928	0.886
	H_t		1.089	
	H_b			1.110
5.450	B	2.003	0.926	0.900
	H_t		1.090	
	H_b			1.107
5.870	B	2.003	0.924	0.906
	H_t		1.092	
	H_b			1.106
$(\infty)BH_3$	B	2.003	0.899	
	H_t		1.119	

[a] The 3.354 distance is that in diborane, and all distances are in au. [b] Populations in parentheses are for the far boron.

The density on the B···B axis has changed substantially from that in B_2H_6. Thus, the (bent) bridge bond does not show substantial covalent formation until the B···B distance has closed to nearly 4 au, corresponding to a B–H distance (far boron) of 3.1 au.

The population analysis (Table IX) and hybridization (population basis, Table X) show that the orbitals remain quite localized as two-center bonds, except, of course, for the gradual formation of the two BH_bB bridge bonds at the short B···B distances (4.334 au and less). Changes in populations and hybridizations of bonds not involved in the reaction are small (note the B–H_t bonds) and thus support arguments for transferability.[27] Trends in the formation of the BH_bB bonds themselves are an overall decrease in contributions from boron 2s and $2p_y$, (axes in footnote *a*, Table X) and a nonlinear increase in hybridization ratio x (in sp^x) on each boron as the B···B distance decreases. The slight peak in the population of the BH_bB bond at the transition state (B···B, 4.61 au) suggests that the small SCF barrier is largely due to repulsions involving those hydrogens which are starting to bridge as $2BH_3$ approach in the C_{2h} geometry. At this distance, our results suggest further that sufficient overlap to give covalent stabilization has not yet developed. A perturbation in the bridge LMO at 4.33 au can be seen in the plots (Figures 4e, 5e, and 6a), but little bonding is found. This conclusion is reinforced by the small change noted in the atomic orbital populations (Table X). A much larger perturbation is seen in the bridge LMO at 3.98 au, and the population analysis at this distance shows the first major change in the electron density of the system. The two borons thus re-

(27) (a) C. Trindle and O. Sinanoglu, *J. Chem. Phys.*, **49**, 65 (1968); (b) *J. Amer. Chem. Soc.*, **91**, 853 (1969); (c) S. Rothenberg, *J. Chem. Phys.*, **51**, 3389 (1969); (d) W. England, L. S. Salmon, and K. Ruedenberg, *Top. Current Chem.*, **23**, 31 (1971).

Table X. Analysis of Localized Orbitals of BH_bB and BH_t Bonds into 2s, $2p_x$, $2p_y$, and $2p_z$ Components[a] for Symmetric Pathway

B–B distance	BH_b 2s	BH_b $2p_x$	BH_b $2p_y$	BH_b p/s[c]	BH_t 2s	BH_t $2p_z$	BH_t $2p_x$	BH_t $2p_y$	BH_t p/s
3.354[b]	0.120	0.186	0.201	3.225	0.338	0.460	0.142	0.0	1.781
3.774 (C)[d]	0.156	0.190	0.232	2.705	0.363	0.462	0.122	0.006	1.625
(F)[e]	0.060	0.149	0.136	4.750					
3.986 (C)[d]	0.226	0.199	0.288	2.155	0.359	0.458	0.103	0.029	1.641
(F)[e]	0.02	0.105	0.077	9.1					
4.334	0.288	0.190	0.353	1.885	0.348	0.455	0.072	0.067	1.706
6.612	0.303	0.188	0.369	1.838	0.346	0.452	0.062	0.079	1.713
5.031	0.318	0.172	0.403	1.808	0.342	0.449	0.048	0.096	1.733
5.451	0.324	0.162	0.421	1.800	0.340	0.447	0.042	0.103	1.741
5.870	0.326	0.172	0.414	1.797	0.339	0.446	0.043	0.102	1.749
(BH_3)					0.328	0.144	0.0	0.433	1.764
					0.328	0.577	0.0	0.0	1.764

[a] The B···B axis is x; the y axis is perpendicular to x and is in the $B–H_b···B$ plane; and the z axis is in the H_tBH_t plane. There is no p_z component to the BH_b bond. [b] This distance refers to the diborane molecule, and all distances are in au. [c] The p/s ratio is given in terms of populations not orbital coefficients of the hybrid. [d] Close (parent) boron. [e] Far boron.

distribute their electron densities among the atomic orbitals of the valence shell as the two bridge bonds are formed. The $2p_x$ orbital on the far boron gains density the fastest even though the $2p_y$ orbital in B_2H_6 has a slightly greater density (axes are given in footnote *a*, Table X). The parent boron $2p_x$ orbital population varies slightly with a slight minimum at 3.98 au. The total $2p_y$ density per bridge LMO on the two borons remains constant (0.35–0.40 electron) with the $2p_y$ orbital on the far boron gaining density. The 2s orbital population increases at a slower rate on the far boron than do the $2p_x$ and $2p_y$ orbital populations. The 2s population per bridge LMO declines with most of the population being transferred to the $2p_x$ orbitals participating in the bridge bond. Thus, a remarkable electron-transfer mechanism on each atom exists as electrons are transferred from the 2s orbital to the $2p_x$ orbital to provide the most stable bonding situation. An analysis of an extended basis set SCF calculation would be more complex, as would be the analysis of the SCF–CI results of the preceding section. However, the localization procedure is no more difficult or lengthy for any type of extended calculation since only integrals over occupied molecular orbitals are used.

Owing to the exponential nature of atomic wave functions, the onset of significant chemical bonding begins within a rather small range of interaction distance. In a previous study[26] of the addition of a proton to the double bond in ethylene, this interaction became substantial at a distance of 4 au between the proton and the center of the double bond on the CC axis. In the incipient diborane molecule the significant interaction H···B distance is substantially less, about 3.1 au. Both reactions form three-center bonds, but the interaction in incipient $C_2H_5^+$ is aided by electrostatic interaction and less hindered by electron repulsions than is the interaction of the B–H bond of one BH_3 with the vacant orbital on boron of the other BH_3 in the transition complex for formation of diborane. Thus, the formation of a three-center covalent bond between two atoms of approximately equal electronegativity occurs at a reasonably short distance of 1.65 Å (3.1 au).

We show in Figure 8 and in Tables IX and X the total density, localized bond density, and population analyses for BH_3 (D_{3h}). Three equivalent localized BH bonds are present, and hybridization at boron is $sp^{1.76}$ on a population basis. Energy quantities for

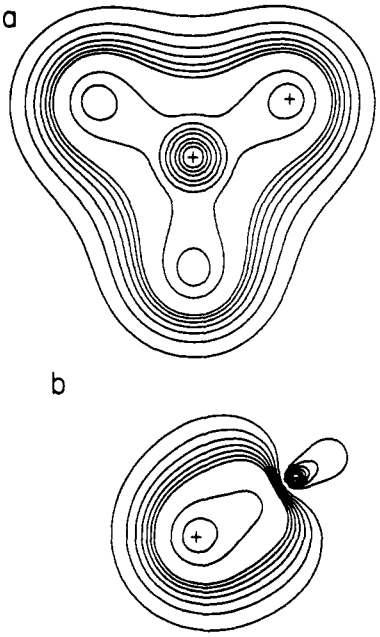

Figure 8. Electron density maps for borane (BH_3). (a) Total electron density. (b) Localized B–H orbital. Contour levels are the same as those in Figure 4. The "+" marks correspond to the unique atomic positions.

BH_3 are given in Table VIII in order to complete the comparison with diborane and the intermediate states of this reaction of two boranes to give diborane.

Finally, the problems which have been treated above are concerned specifically with transition states in which distances are substantially different from those of ground states of reactants or products. In transition states which have molecular parameters more nearly like those of the ground state, for example the barrier to internal rotation in ethane, the SCF approximation is often good even with a minimum basis of Slater atomic orbitals.[28]

Acknowledgment. We thank the Office of Naval Research for support of this research. We also thank R. M. Stevens for the use of his SCF program and D. S. Marynick, D. Kleier, and T. Halgren for many helpful discussions.

(28) R. M. Pitzer and W. N. Lipscomb, *J. Chem. Phys.*, **39**, 1995 (1963).